

Rheological Properties of Oppositely Charged Polyelectrolyte–Surfactant Mixtures: Effect of Polymer Molecular Weight and Surfactant Architecture

Ioannis S. Chronakis^{*,†,‡} and Paschalis Alexandridis^{†,§}

Physical Chemistry 1, Center for Chemistry and Chemical Engineering, Lund University, Box 124, S-221 00 Lund, Sweden; The Swedish Institute for Fibre and Polymer Research, Department of Basic Research, Box 104, SE-431 22 Mölndal, Sweden; and Department of Chemical Engineering, University at Buffalo, The State University of New York, New York 14260-4200

Received April 6, 2000; Revised Manuscript Received March 19, 2001

ABSTRACT: We report on the gel formation and resulting rheological properties in aqueous solutions of cationic cellulose ether polymers of “high” (JR30M) and “low” (JR400) molecular weight (MW), upon the addition of anionic surfactants of different architecture but with the same charge (sodium dodecyl sulfate, SDS, sodium dodecylbenzenesulfonate, SDBS, and sodium bis(2-ethylhexyl) sulfosuccinate, AOT). From the comparison of systems with the same charge density and ratio but different (polymer) MW and (surfactant) architecture, we assess the nature of the interactions leading to gel formation as well as structural properties of the polymer–surfactant aggregates. In the high-MW polyelectrolyte–surfactant systems, polymer-dependent cross-links and chain entanglements are observed, while the surfactant architecture plays a secondary role. For example, the slope of the double-logarithmic plot of the increase in viscosity with surfactant concentration is the same with any of the three surfactants. Surfactant-dependent cross-links are obtained for the low-MW polyelectrolyte–surfactant complexes, and the surfactant architecture and the hydrophobic effect are responsible for the cooperativity of the cross-links. The slope of the viscosity vs surfactant concentration data is much higher in the case of low-MW polymer. The similarities and the differences in the viscoelastic properties for a polymer or a surfactant-controlled cross-linking mechanisms are discussed.

Introduction

Polymers that dissolve in or swell with water find use in a great variety of products (e.g., cosmetics and pharmaceuticals) and processes (e.g., extraction of petroleum and processing of minerals). Many applications of water-soluble polymers arise from their ability to modify the rheological properties of media in which they are present. Water-soluble polymers are often used in conjunction with surfactants.^{1–6} Of particular interest are systems containing oppositely charged polymers and surfactants. The interactions between polyelectrolytes (PE) and surfactants (S) of opposite charge have been characterized in considerable detail over the recent years.^{7–11} Polyelectrolyte–oppositely charged surfactant complexes form as a result of an electrostatic attraction between the charged headgroup of the surfactant and the ionized units of the polymer, although hydrophobic interactions also play a role.^{9,12,13} It is well-known that in polyelectrolyte–surfactant complexes surfactant molecules aggregate and form intramolecular micelles. This aggregate formation is the necessary condition for the formation of such complexes.^{9,12,14} Due to the strong attraction between the two species (PE and S), their interaction commences at very low surfactant concentrations. This association is cooperative and occurs at a surfactant concentration well below its critical micelle concentration (cmc) observed in the absence of PE. The term critical aggregation concentration (cac) is used to indicate the onset of surfactant association in the

presence of PE.^{9,15–18} Above cac, the surfactant molecules self-assemble on the polymer to form aggregates with a relatively low charge (as compared to free surfactant micelles). It has been shown that the morphology of the polymer–surfactant complex micelles differs from that of the corresponding “free” surfactant micelles.¹⁹ Usually, these aggregates are smaller in size than “free” micelles.^{16,17}

Polyelectrolyte solutions exhibit behavior remarkably different from solutions of uncharged polymers.^{20,21} Moreover, the aqueous solution properties of PE can be dramatically changed with the presence of added oppositely charged surfactants. For example, these interactions can lead to a large increase in solution viscosity^{12,13,22–25} or in some cases to phase separation.^{26,27} Goddard and co-workers²⁸ have reported that when an anionic surfactant, such as sodium dodecyl sulfate (SDS), sodium dodecylbenzenesulfonate (SDBS), or sodium bis(ethylhexyl) sulfosuccinate (AOT), was added to a cationic cellulosic polymer, a great increase in apparent viscosity occurred. Indeed, formation of strong, clear aqueous gels was obtained at quite low levels of polymer (about 1%) with the surfactant at about one-tenth of this concentration. In a homologous series of cationic cellulose polymers with low and high molecular weight (MW), mixed in aqueous solution with SDS at the optimal gelling ratio, the elastic modulus increased (i) with the polymer molecular weight and (ii) with the degree of cationic substitution. Moreover, in a mixture with the highest MW polymer, gelling efficiency followed the order SDS \gg SDBS \approx AOT. A number of other publications deal with the behavior of PE–oppositely charged surfactant systems at dilute solutions, and evidence of structural changes accompanying

[†] Lund University.

[‡] The Swedish Institute for Fibre and Polymer Research.

[§] University at Buffalo, The State University of New York.

* Author for correspondence: Tel + 46 31 706 63 00; Fax + 46 31 706 63 63; E-mail ioannis.chronakis@ifp.se.

the formation of the "complexes" has been obtained from measurements such as self-diffusion²⁹ and small-angle neutron scattering.²³ It is generally accepted that the PE-S interactions are enhanced for a surfactant of longer hydrocarbon tail.^{9,30} The surfactant chain length dependence for the formation of the aggregates is similar to the alkyl chain length dependence for the formation of surfactant micelles.^{9,12} Moreover, the properties of PE also play a major role in complex formation. Perhaps the most fundamental parameter characterizing the PE is the linear charge density, ξ . Generally, an increase in ξ causes a stronger interaction.⁹

Despite the progress made, a systematic investigation on the complex formation and structures between polyelectrolyte and oppositely surfactant is still needed. The general dependencies of the polymer type, molecular weight, concentration, and charge density which influence these PE-S interactions are not fully understood yet. At the same time the effects of the chemical structure of surfactants with similar charge but with different hydrocarbon tails or branched type, which determine the range of interactions, still remain to be examined. In addition, despite its significance on applications, very few studies have been devoted to the rheological behavior and to the characteristic structural parameters of these macromolecular complexes. In this investigation we study the viscoelastic rheological properties of cooperative cross-linked networks consisting of positively charged cellulosic polymer (of two different molecular weights) and anionic surfactants (having the same charge, but different architecture and different hydrophobic interactions). On the basis of oscillatory frequency measurements, we derive slopes that compare how the elastic modulus, the complex viscosity, and the relaxation time vary with the surfactant concentration and the polymer molecular weight. Our approach was also extended to the flow behavior and to the nonlinear viscoelastic properties of oppositely charged PE-S complexes. We describe the effect of the shear rate and the resulting slopes of the Newtonian viscosity vs surfactant concentration data and the applicability of the Cox-Merz rule and we also compare the flow properties of the PE-S mixtures with respect to the cmc of surfactants. Finally, we discuss the polymer- and surfactant-dependent cross-linking mechanisms for PE-S complexes and summarize the similarities and the differences in the viscoelastic properties observed. Such characteristics have received up to now little attention in the literature.

Materials and Methods

Materials. The cationic polymers JR400 (lot JD6103) and JR30M (lot BC1003X) examined here were supplied by Amerchol, Union Carbide Chemicals, and Plastics Company, USA. They were used after purification by dialysis against Milli-Q-treated water in a Filtron Ultraset device, followed by lyophilization. Both JR30M and JR400 are the chloride salt of the *N,N,N*-trimethylammonium derivative of hydroxyethylcellulose (quaternized hydroxyethylcellulose, HEC) (Figure 1). JR400 has a molecular weight of approximately 400 000–500 000.^{31,32} An aqueous solution of 1 wt % polymer bears a charge concentration of 10 mM, and the mean contour length between charges is about 20 Å.^{31,32} JR30M has a molecular weight of about 700 000–1000 000 and the same charge density as JR400.^{28,33} The degree of quaternization (from nitrogen content), determined by using the Kejlhdal method, was found to be 33 and 29 (number of charges per 100 monosaccharide units) for the JR30M and JR400, respectively.³³ Note that we call JR30M a "high"-MW polymer and JR400 a "low"-MW polymer.

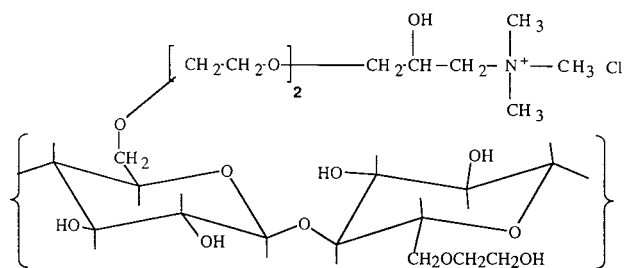


Figure 1. Nominal chemical structure of the cationic hydroxyethylcellulose polymers JR30M and JR400.

Anionic single-tail surfactant sodium dodecyl sulfate (SDS), especially pure, was purchased from BDH Chemicals and used as received. The cmc of SDS is 8.3 mM in pure water.³⁴ Anionic benzene surfactant, sodium (linear) dodecylbenzenesulfonate (SDBS), was purchased from Tokyo Kasei. The specific linearity that Tokyo Kasei claimed was not confirmed by ¹H NMR in DMSO-*d*₆. Instead, the surfactant is found to be partially branched and a mixture of various compounds. The main part (95%) is monosubstituted benzene ring with probably many different combinations. The cmc of SDBS is at 1.2 mM in pure water.³⁵ The anionic double-tail surfactant sodium bis(ethylhexyl) sulfosuccinate (Aerosol OT) was purchased from Sigma. The cmc of AOT is at 2.5 mM in pure water.³⁶

Sample Preparation. All samples were individually prepared by mixing appropriate aqueous stock solutions of polymer and surfactant at different ratios to achieve the desired final composition. The water used was of Milli-Q quality. The mixtures were homogenized by stirring or by centrifugation in alternating directions (in the case of viscous samples) and then left to equilibrate at 25 °C for at least 1 week. After equilibration, the samples were centrifuged for at least 24 h, and the phase behavior was determined by visual inspection. One-phase samples are homogeneous and clear, often highly viscous gels. All the samples discussed here are one-phase. Most of the two-phase samples displayed two well-separated isotropic phases.

Low-Amplitude Oscillatory and Flow Rheological Measurements. Rheological measurements under low-amplitude oscillatory shear were performed on a controlled stress Carri-Med CSL100 rheometer (TA Instruments, UK) using a solvent trap cone-parallel plate geometry (stainless steel 40 mm radius; 27 μm separation) at a frequency range of 20–10^{−3} Hz. All oscillatory measurements were performed with 0.5% strain since strain sweeps on selected gels demonstrated that the working deformation was well within the linear viscoelastic region. The oscillatory measurements allowed recording of the storage modulus (*G'*), the loss modulus (*G''*), $\tan \delta (= G''/G')$, and the complex viscosity ($\eta^* = (G'^2 + G''^2)^{1/2}/\omega$) as a function of the frequency of oscillation ω . Following the oscillatory measurements, all samples were subjected to flow measurements, and the shear viscosity (η) was recorded as a function of the shear rate at 25 °C.

As mentioned in the Introduction, the viscoelasticity of the above PE-S mixtures was first reported by Goddard and co-workers,²⁸ and rheological parameters such as the elastic modulus, $\tan \delta$, and some shear rate measurements were presented. However, both JR30M and JR400 polymers used in that work most likely contained salt impurities which can affect the electrostatic interactions. Careful purification of the polymers by dialysis was applied in our study. Moreover, a complete rheological characterization involving oscillatory measurements and shear flow measurements is presented here.

Results and Discussion

Frequency Dependence. 1 wt % JR30M polymer forms in water a viscoelastic solution which has high-frequency dependence of both *G'* and *G''* (Figure 2a). The crossover frequency is about 7 Hz, a value very close to that of 5 Hz reported by Goddard et al.²⁸ However,

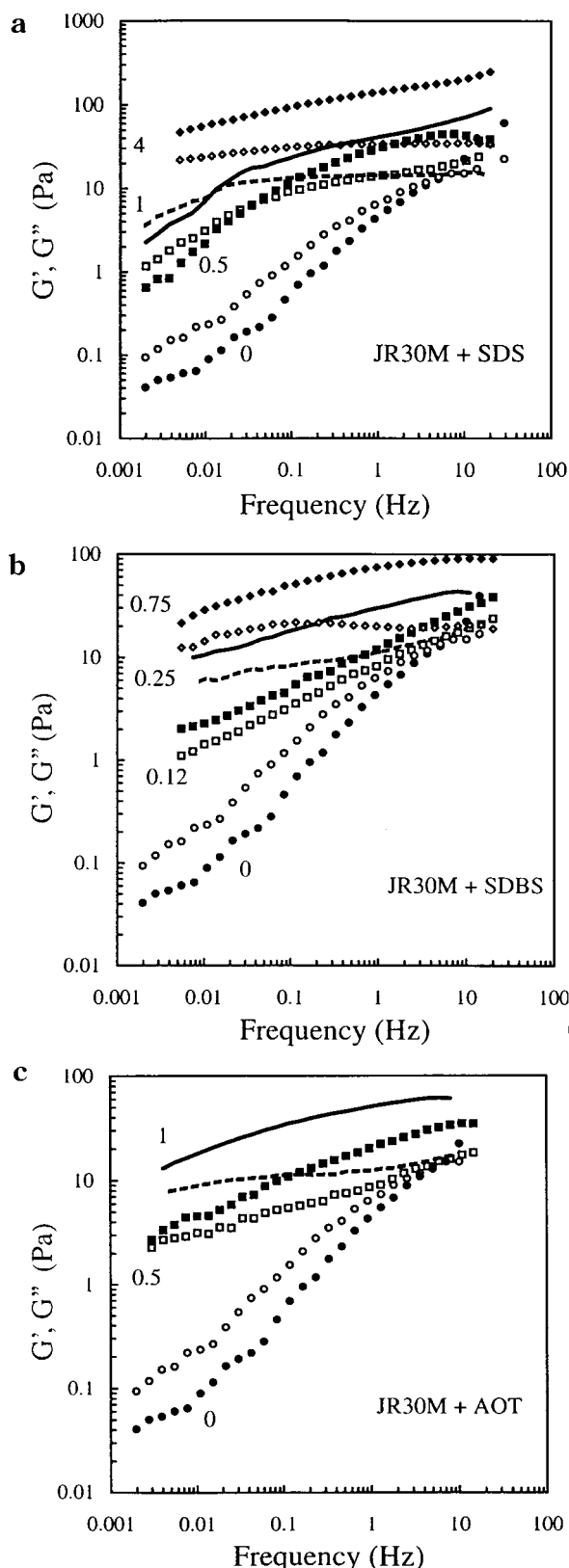


Figure 2. Frequency dependencies of G' (filled symbols) and G'' (open symbols), obtained from oscillatory rheological measurements, for 1 wt % JR30M with various surfactant concentrations: (a) G' (●) and G'' (○) for 0 mM SDS; G' (■) and G'' (□) for 0.5 mM SDS; G' (—) and G'' (---) for 1 mM SDS; G' (◆) and G'' (◇) for 4 mM SDS. (b) G' (●) and G'' (○) for 0 mM SDBS; G' (■) and G'' (□) for 0.12 mM SDBS; G' (—) and G'' (---) for 0.25 mM SDBS; G' (◆) and G'' (◇) for 0.75 mM SDBS. (c) G' (●) and G'' (○) for 0 mM AOT; G' (■) and G'' (□) for 0.5 mM AOT; G' (—) and G'' (---) for 1 mM AOT (25 °C, 0.5% strain).

in the presence of 0.5 and 1 mM SDS (Figure 2a) a weak gel-like system is obtained with a high-frequency dependence of G' and G'' up to the crossover frequency. Beyond that, G'' remains relatively constant and reaches a plateau, denoting a constant viscous relaxation, while G' shows a progressive increase with the frequency and no plateau value is obtained. Similar behavior of both moduli is observed with the addition of higher surfactant concentrations. Clear one-phase solutions are obtained up to addition of 6 mM SDS in 1 wt % JR30M. The mechanical properties for representative JR30M solutions in the presence of SDBS are shown in Figure 2b. The addition of fairly low amount of surfactant (0.12 mM) results in a weak gel-like system where G' is always higher than G'' . Both moduli are highly frequency dependent and increase in a parallel manner with increasing frequency of oscillation. No crossover frequency could be obtained for the JR30M–SDBS complexes. Moreover, addition of a higher amount of SDBS resulted in a gel-like system with G' increasing progressively with frequency while G'' is relatively less frequency-dependent (Figure 2b). The addition of up to 1 mM SDBS in 1 wt % JR30M resulted in monophasic systems. Similar viscoelastic properties are also observed by the addition of the double-tailed surfactant AOT to JR30M (Figure 2c). The moduli become higher as the surfactant concentration is increased. One-phase solutions are obtained up to 4 mM AOT in 1 wt % JR30M.

1 wt % JR400 aqueous solution in the absence of surfactant has a low viscosity and was not studied by oscillation rheology. However, the mixtures of 1 wt % JR400 with SDS (Figure 3a) display a weak gel-like behavior, typical of entangled network systems with weak cross-links, in agreement with recent results by Tsianou and Alexandridis.²⁵ The crossover frequency can be measured and moves to lower values as the surfactant concentration is increased. One-phase systems are obtained up to addition of 6 mM SDS in 1 wt % JR400, a similar surfactant concentration as in the case of JR30M–SDS. The addition of SDBS to JR400 solution causes as well a significant enhancement in storage and loss moduli and affects strongly the viscoelastic character (Figure 3b). One-phase solutions are obtained up to 4 mM SDBS in 1 wt % JR400, 3 mM more than in the case of the JR30M–SDBS system. Note that the JR400–SDBS behavior differs from that of JR30M–SDBS: lower moduli and crossover frequency are observed in the case of low-MW polymer. Figure 3c shows the behavior of JR400 solution with added AOT. The moduli are substantially lower than in the case of JR30M–AOT complexes, and the crossover frequencies can be measured in the case of the low-MW JR400–AOT mixtures. The G'' continuously increases at low amounts of surfactant; however, at higher concentrations (i.e., 3.5 mM AOT, Figure 3c) G'' remains constant at frequencies above the crossover point. Monophasic solutions are reached with 5 mM AOT.

We must note that the polymer charges are always in excess; 1 wt % JR30M or 1 wt % JR400 aqueous solutions bear a charge concentration of 10 mM. Therefore, the highest surfactant concentration used in our work, 4 mM SDBS, 4 mM AOT, and 6 mM SDS, is in terms of charge density about 2 times lower than that of the polyelectrolyte. This is reasonable since the strong electrostatic interaction between PE and S causes precipitation when the concentration of surfactant is

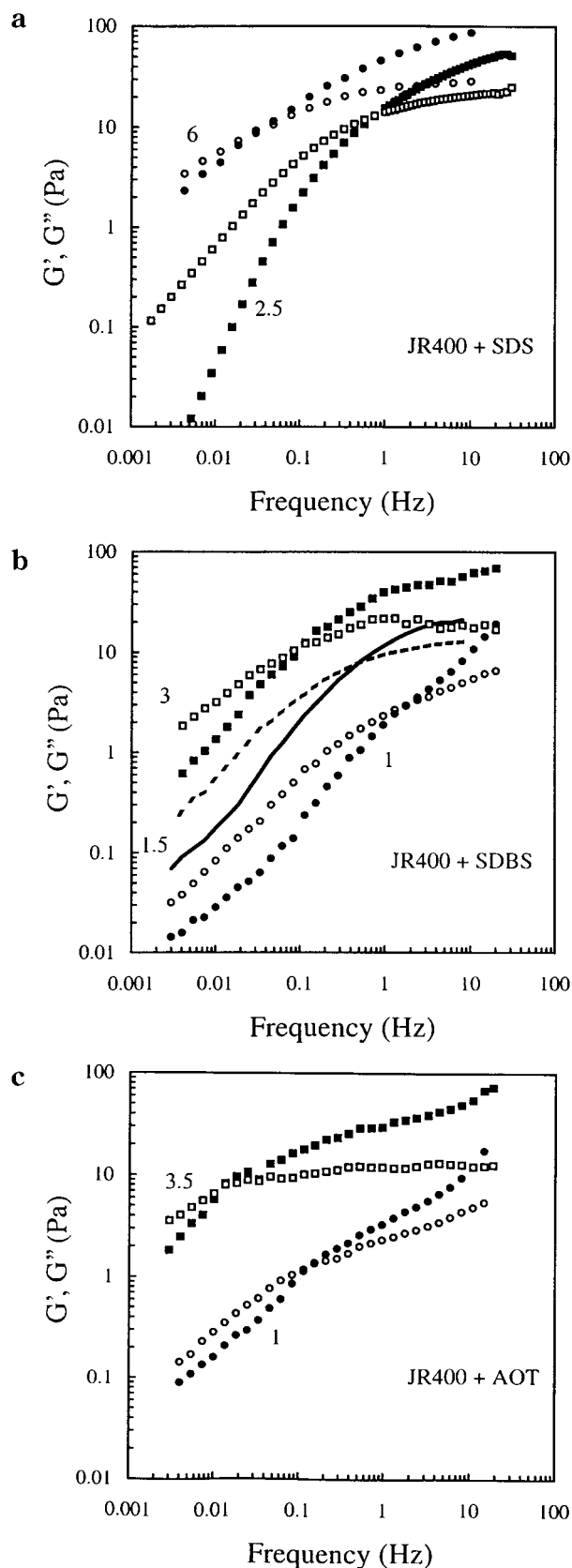


Figure 3. Frequency dependencies of G' and G'' (same as in Figure 2), obtained from oscillatory rheological measurements, for 1 wt % JR400 with various surfactant concentrations. (a) G' (■) and G'' (□) for 2.5 mM SDS; G' (●) and G'' (○) for 6 mM SDS. (b) G' (●) and G'' (○) for 1 mM SDBS; G' (—) and G'' (---) for 1.5 mM SDBS; G' (■) and G'' (□) for 3 mM SDBS. (c) G' (●) and G'' (○) for 1 mM AOT; G' (■) and G'' (□) for 3.5 mM AOT (25 °C, 0.5% strain).

increased. Moreover, the results discussed above involve systems with surfactant concentration below (in the case of SDS) and higher (SDBS, AOT) than their cmc in pure water.

The plots of G'' against G' (Cole–Cole plots) are not semicircular for both JR30M– and JR400–surfactant mixtures (plots not shown here). The distorted circular shape suggests that the relaxation, as characterized from the frequency dependence, is not a single well-defined process but has some distributions of the relaxation time.³⁷ In addition, the observed plateau of G'' after the crossover point indicates another (probably slower) relaxation mode. The Maxwell model (a spring and a dash pot in a series) also fails to describe the data well, and this may indicate that strong intermolecular associations give rise to highly entangled systems. At present we do not have a theoretical model for the interpretation of the experimental observations shown in Figures 2 and 3.

Elastic Modulus and Complex Viscosity. A convenient way to summarize the moduli vs frequency results of Figures 2 and 3 and to show the effect of added surfactant is to plot the moduli vs the surfactant concentration at a fixed frequency. The G' value at 1 Hz, which reflects the cross-linking density of the viscoelastic systems at this frequency, is plotted as a function of the surfactant concentration in Figure 4a–d. The curves for both JR30M and JR400 polymer–surfactant systems exhibit the same general trends, with the elastic moduli increasing with increasing surfactant concentration (more than 2 orders of magnitude greater than the polymers alone). Obviously, the cross-link density is the same for both JR30M and JR400 polymer–surfactant systems (since the concentrations and charge densities are the same), but the strength of association is increased in the case of the high-MW polymer since there are more cross-links per polymer chain.

An optimal elastic modulus enhancement occurs at 2.5 mM SDS in 1% JR30M. Beyond that, further addition of surfactant leads to a gradual loss of cross-links and decrease in elastic modulus up to 5 mM of SDS. For the JR400–SDS complexes, an optimal elastic modulus is obtained with 4 mM of surfactant, but this modulus value is nearly 3 times lower than that of 2.5 mM SDS–JR30M mixture. The association behavior of JR30M–SDBS showed a monotonic increase of G' at 1 Hz up to 1 mM of SDBS, while for the JR400–SDBS system an optimal elastic modulus enhancement is observed at 3 mM surfactant. The modulus of JR400–SDBS network almost collapsed with the addition of 4 mM SDBS. The elastic moduli of JR30M–SDBS are 10 times higher than the one with the low-MW polymer with the same surfactant. For the JR400–SDBS complex, it is notable the effective increase in G' between 1 and 2 mM (the cmc of SDBS is 1.2 mM), suggesting that the junctions may be micelle-like in some cases but not in others. Note also the difference in the solubility limit of SDBS with the high- and low-MW polymer, 1 and 3 mM, respectively, while with SDS no differences are found. As has already been mentioned, SDBS has a cmc about 7 times lower than that of SDS. In the case of AOT a monotonic increase of G' at 1 Hz is observed for both polymer systems, although the elastic moduli of JR30M–AOT are about 6 times higher than those with JR400 at the same AOT concentration (Figure 4a–d). A maximum in the elastic modulus is obtained at 4 and

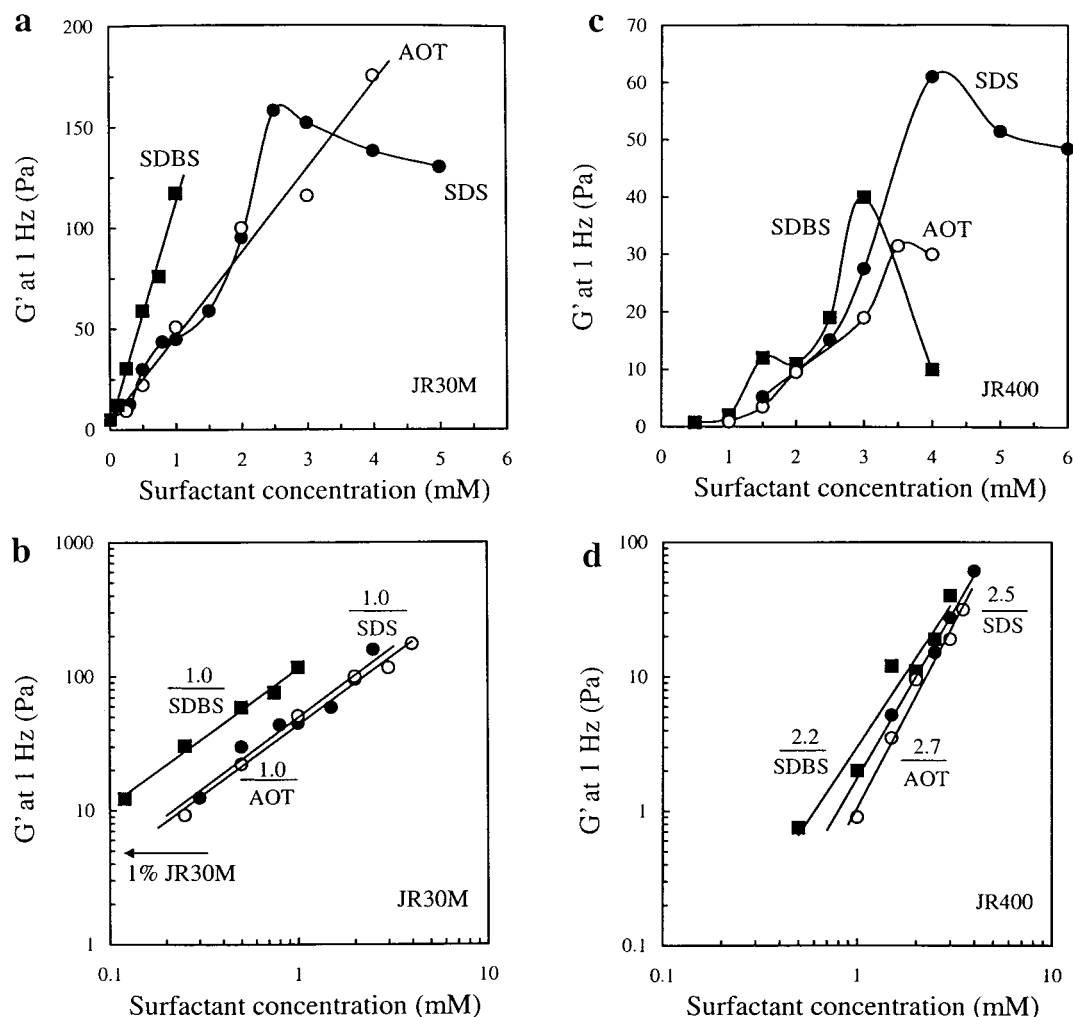


Figure 4. Variation of the elastic modulus G' (measured at 1 Hz) with surfactant concentration for (a) 1 wt % JR30M with SDBS (■), SDS (●), and AOT (○). (b) JR30M with surfactants plotted on a log–log scale. The arrow shows the G' (measured at 1 Hz) for 1 wt % JR30M without surfactant addition. (c) 1 wt % JR400 with SDBS (■), SDS (●), and AOT (○). (d) JR400 with surfactants plotted on a log–log scale.

3.5 mM of AOT for the high- and low-MW polyelectrolyte, respectively.

Our results are in close agreement with the previous findings of Goddard and co-workers;²⁸ however, the maximum modulus at a frequency of 0.2 Hz was observed at 5.2 mM for JR30M–SDS and at 2.9 mM for JR30M–SDBS. Nevertheless, it cannot be ignored that in this previous study the cellulosic polymers may contain salt impurities, and also the chemical structure of the commercial SDBS surfactant was not examined. Maximum in the modulus when water-soluble polymers are mixed with surfactants has been observed previously also for other HEC–S systems.^{38,39} Drye and Cates⁴⁰ have also discussed this behavior in pure surfactant systems where the viscosity increases and then starts to fall dramatically again after a certain parameter (water content or counterion strength) moved further in the same direction.

In Figure 4b,d we plot the elastic moduli data (from Figure 4a,c) up to the maximum modulus value as a function of the surfactant concentration in a logarithmic scale. Our aim is to compare data from the different PE–S systems. By comparing parts b and d of Figure 4, it is clear that the elastic modulus increment of the JR400–S mixtures is sharper and steeper (slopes between 2.2 and 2.7) than the behavior found for the

JR30M–S mixtures. (The slope is 1.0 for all systems examined even though the surfactant architecture of the systems is very different.) We will return to these results below; again we emphasize the quite different behavior of the high- and low-MW polymer with the surfactants.

We now introduce in the discussion the complex viscosity (η^*) which allows us to compare both elastic and loss moduli with frequency of oscillation and to correlate these data with the Newtonian viscosities and shear flow results presented below. Figure 5a,c shows the complex viscosity at different frequencies plotted against the surfactant concentration (c). In a log–linear plot for both JR30M–S and JR400–S mixtures, η^* initially increases substantially with the surfactant concentration at all frequencies and then remains relatively constant, as shown in Figure 5a. Furthermore, the concentration dependence of the complex viscosity before the plateau when plotted in a log–log scale shows a strong increase with surfactant concentration (Figure 5b,c). The magnitude of increase can be expressed with the slope of the log–log plot; while the log–log plot is not perfectly linear in this case, the slope aids in comparing data from different systems. The slopes observed for the JR30M–S systems are reported in Table 1 and have distinct values for each frequency. It

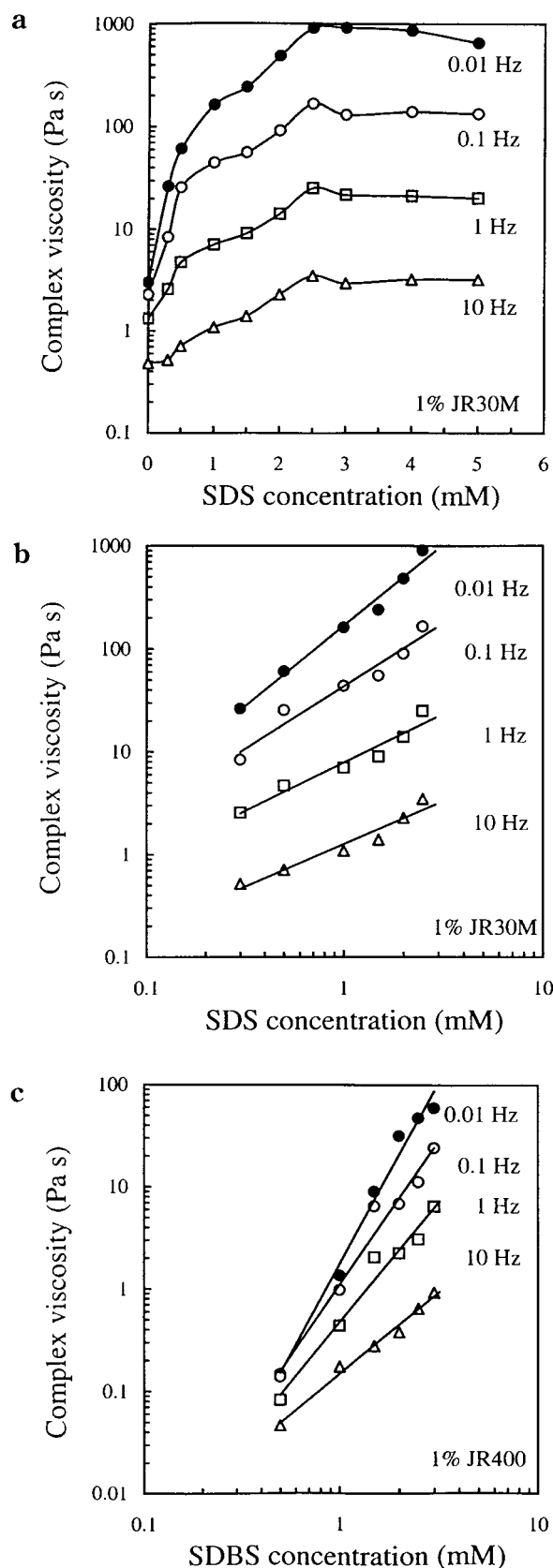


Figure 5. Variation of the complex viscosity (η^*) (measured at different frequencies) with surfactant concentration for (a) 1 wt % JR30M-SDS and (b) 1 wt % JR30M-SDS on a log-log scale and (c) 1 wt % JR400-SDBS on a log-log scale.

is notable that, at a certain frequency, the slope for all JR30M-S complexes is the same, even though the surfactant architecture of the systems is very different.

Table 1. Values of the Slopes, Obtained at Different Frequencies, from the Double-Logarithmic Plot of the Concentration Dependence of the Complex Viscosity (η^*) of 1 wt % JR30M and 1 wt % JR400 with SDS, SDBS, and AOT Surfactants

freq (Hz)	1 wt % JR30M			1 wt % JR400		
	SDS	SDBS	AOT	SDS	SDBS	AOT
0.01	1.6	1.4	1.6	3.8	3.6	3.8
0.1	1.2	1.1	1.0	3.0	2.8	2.9
1	0.9	0.9	0.9	2.3	2.4	2.4
10	0.8	0.6	0.7	1.6	1.6	1.7

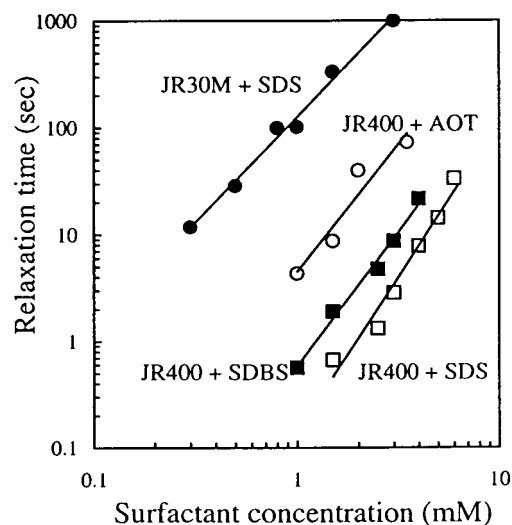


Figure 6. Changes in the relaxation time as a function of surfactant concentration for 1 wt % JR30M-surfactant and 1 wt % JR400-surfactant systems: JR30M-SDS (●), JR400-AOT (○), JR400-SDBS (■), and JR400-AOT (□).

When the molecular weight of the polymer decreased, in the case of JR400-S, the concentration dependence on viscosity is much stronger (about 2.5 times higher) as illustrated in Figure 5c. The slope at a given frequency still remains almost the same for all JR400-SDBS, -AOT, and -SDS mixtures (Table 1).

The distinct values of the slopes for the complex viscosity are the result of distinct and different mechanisms for the decay of the structural entanglements for each low- and high-MW PE-S mixture. The high-MW polymer JR30M exhibits a lower concentration dependence and a more cross-linked association (higher viscosity and G') in comparison with the low-MW polymer. This could be attributed mainly to *polymer-dependent* cross-links and chain entanglements, which are less subjected to the surfactant-controlled cross-link mechanism. The higher concentration dependence of the η^* in JR400-S compared with JR30M-S composites most likely reflects a more cooperative cross-linking behavior originating from the *surfactant-controlled* cross-linking mechanism.

Dynamics. A simple way to address some dynamic aspects of the complexes is to look at the frequency of intersection of elastic and loss moduli. We can regard this crossover frequency as a measure of an effective junction lifetime. (This does not exclude the existence of junctions of shorter and longer lifetimes.) Thus, the relaxation time ($\tau = 1/2\pi\omega$) estimated from the frequency of intersection between G' and G'' is plotted as a function of surfactant concentration in Figure 6. As expected, the relaxation time of the network is shifted toward longer times (lower frequencies, slow dynamics)

as the surfactant concentration is increased.^{25,41} An extremely long relaxation time (about 1000 s) is observed for the JR30M–SDS system at relatively high surfactant concentrations (3 mM). The networks of the high-MW polymer exhibit slow dynamics, and we cannot experimentally detect the relaxation times for the case of the branched surfactants AOT and SDBS. The long relaxation time could be ascribed to the strong association of the JR30M–S complexes and may also be related to the slow dissociation of the associated complex domain. Therefore, the presence of these branched surfactants increases substantially the cross-linking density and the lifetime of the junctions. The “stiff” backbone of the cellulose ether polymer chain also contributes to the entanglements. In contrast to JR30M–S, the JR400–SDBS, –AOT, and –SDS systems have a much faster relaxation behavior and shorter relaxation times (between 1 and ≈ 2 orders of magnitude lower), so the surfactant response of the relaxation times can be clearly estimated. We observed that the mixtures with the branched chain surfactants (AOT and SDBS) have much slower dynamics than the JR400–SDS complexes, and the relaxation time increases in the order AOT > SDBS > SDS.

We find that the relaxation time increases with surfactant concentration and the magnitude of increase can be expressed with the slope of the log–log plot for both JR30M and JR400 systems. The slopes are 2.9, 2.5, and 2.4 for the JR400–SDS, JR400–SDBS, and JR400–AOT complexes, respectively. Note that while the relaxation time in the JR400–S mixtures increases in the order of AOT > SDBS > SDS, the slopes show an opposite trend: SDS > SDBS > AOT. The slope, however, for the JR30M–SDS is 2.0, a value again lower than that of JR400–S systems slopes. This behavior is also in accordance with the trends of lower concentration dependence of the complex viscosities of the JR30M–S mixtures (Table 1).

Our results fall in the range of the scaling exponents 3.4–0.58 calculated by Cates and co-workers of the terminal time with the volume fraction (ϕ) of wormlike surfactant micelles in the presence of bond, end-interchange, and reversible scission reactions in the regime where micellar reactions are rapid on the time scale of reptation.⁴² While we cannot theoretically explain the slopes we observed in our PE–S mixtures, it is certain that the size distribution of the entangled “aggregates” (as they break and re-form) and their length are going to affect the time constants for the disentanglement processes. We note that usually in polymer systems comparison of the relaxation time is done with varying the polymer concentration.^{31,39} However, here we examine the slopes with surfactant concentration, which is worth to exploring since the surfactant addition increases the number of entanglements just as they are increased by the polymer concentration.

In what follows we use the word *aggregates* to indicate the surfactant and/or polymer aggregates (caused by chain entanglement) or self-assemblies which form cross-links with the PE. Aggregates in PE–S systems have been found previously for example by fluorescence measurements.⁴³ In our system the substantial evidence which suggests the presence of aggregates is the response of the mixtures.

Flow Behavior and Nonlinear Viscoelasticity. *Effect of Shear Rate.* Following an examination of the

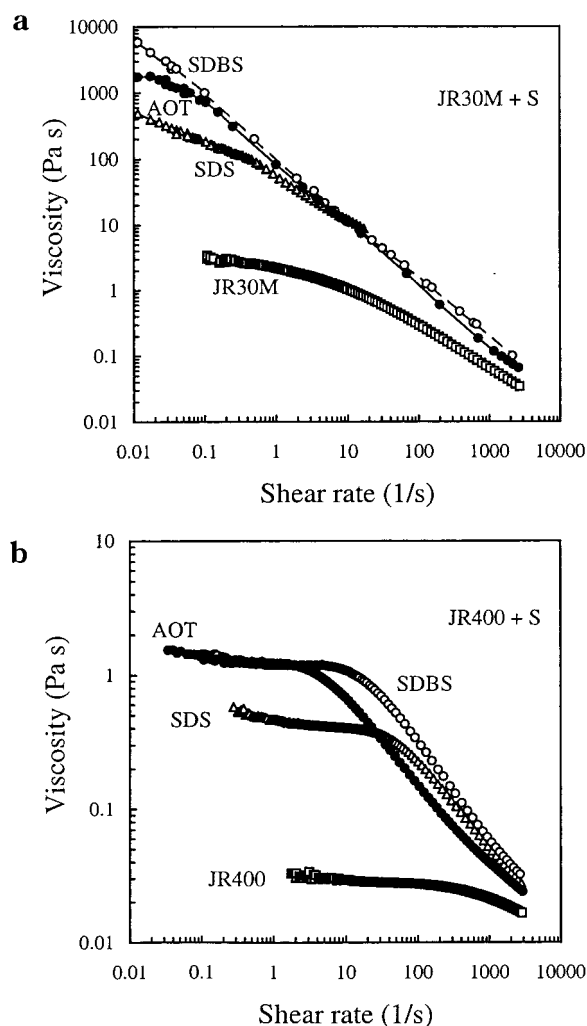


Figure 7. Flow curves (25 °C) (a) for 1 wt % JR30M (\square), 1 wt % JR30M with 1 mM of SDS (\triangle), 1 wt % JR30M with 1 mM AOT (\bullet), and 1 wt % JR30M with 1 mM SDBS (\circ) and (b) for 1 wt % JR400 (\square), 1 wt % JR400 with 1 mM SDS (\triangle), 1 wt % JR400 with 1 mM SDBS (\circ), and 1 wt % JR400 with 1 mM AOT (\bullet).

rheological response at low deformation, we now examine our PE–S complexes at large deformations under shear. All PE–S samples exhibited reversible shear thinning behavior. The shear rate dependence of the apparent viscosity is shown in Figure 7a,b for both polymers (at 1 wt %) with 1 mM of surfactant. As expected, JR30M shows a higher viscosity than JR400, denoting a higher degree of intermolecular entanglement. The Newtonian plateau of JR400–surfactant mixtures could be attained for about 3 orders of magnitude of the shear rate (0.01 – 10 s $^{-1}$). However, the Newtonian region is not attained experimentally for the JR30M–surfactant systems, which all show a pronounced shear thinning behavior and a strong shear rate dependency on the viscosity. A decrease in viscosity with increasing shear rate has usually been assumed to be due to a reduction in the extent of three-dimensional network structure in the polyelectrolyte systems. Most gels based on physical association are indeed shear sensitive.^{5,44,45} In the non-Newtonian regime, the critical shear rate ($\dot{\gamma}_c$) at which the shear thinning occurs decreases in the order of SDS < SDBS < AOT for the JR400–surfactant mixtures (see Figure 7b). Physically the “longer” the aggregate, the easier is

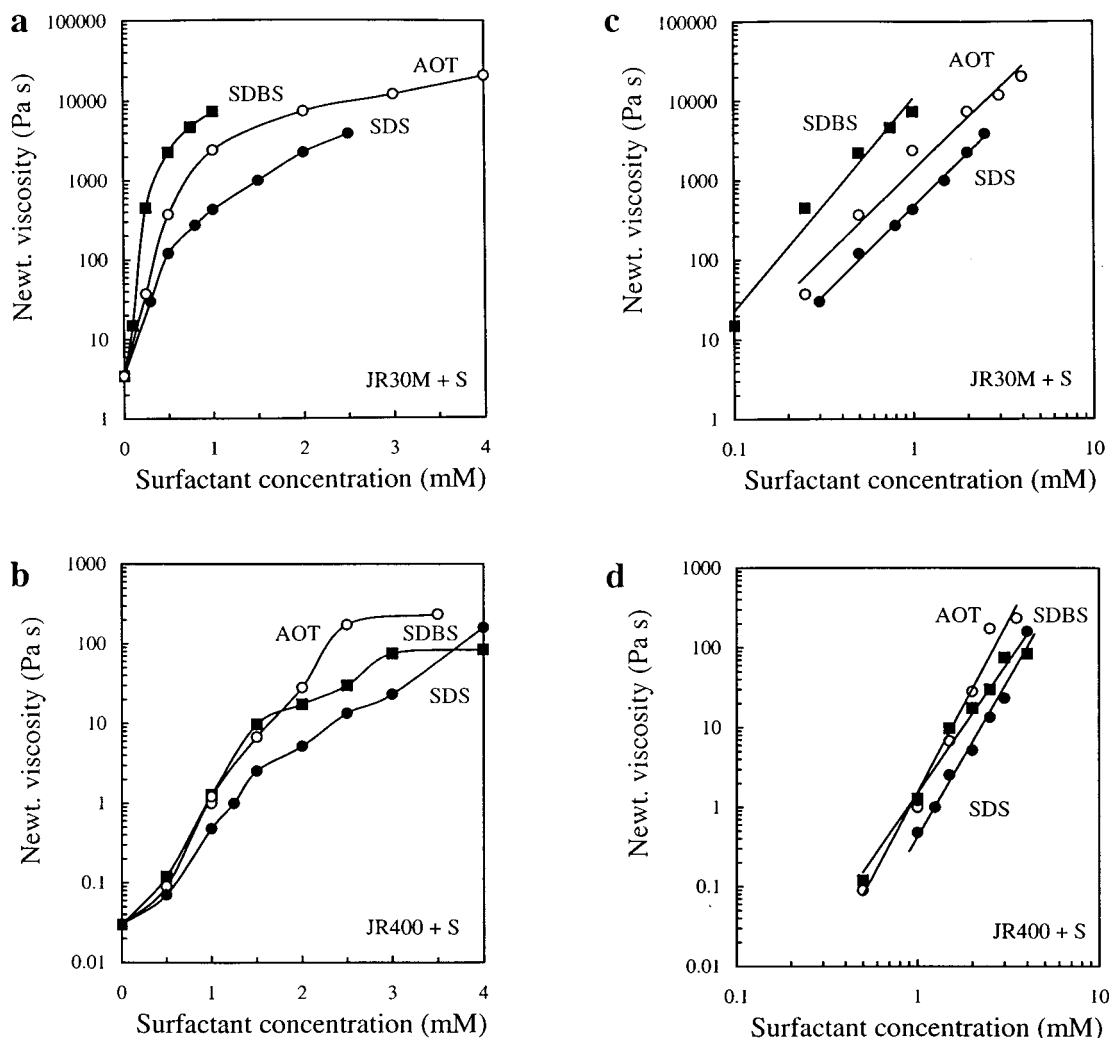


Figure 8. Variation in the Newtonian viscosities (25 °C) as a function of surfactant concentration for (a) 1 wt % JR30M–surfactant systems in linear and (c) in logarithmic scale and for (b) 1 wt % JR400–surfactant systems in linear and (d) in the logarithmic scale. SDS (●), SDBS (■), and AOT (○).

their alignment in the shear flow. Therefore, the PE–S aggregate size increases in the reverse order (AOT > SDBS > SDS) in accordance with our observations from the relaxation behavior in dynamic oscillation. Such conclusion is not very obvious for the JR30M–surfactant complexes because the Newtonian regime has not been attained (see Figure 7a). However, for all JR30M– and JR400–surfactant systems the critical shear rate decreases with increasing surfactant concentration.

It is notable that at such very highly viscous systems, or better gels, it is not easy to detect and record the Newtonian viscosity. We have tried to overcome this (and compare in the same manner all the systems) by utilizing the simplified Cross equation for all systems. All the flow curves are fitted accurately (regression coefficient between 0.94 and 0.99) by the simplified Cross equation which involves three adjustable parameters:⁴⁶

$$\eta = 1/(1 + k\dot{\gamma}^\alpha) \quad (1)$$

where η is the zero shear rate viscosity, $\dot{\gamma}$ is the shear rate, k is the consistency, and α is the shear rate index. Cross found that often a good fit to experimental data was obtained for $\alpha = 2/3$ or $\alpha = 4/5$. For our systems we have obtained both values for α . (The value of $4/5$ is

obtained mostly at high surfactant concentrations.) No systematic dependence of α with the surfactant concentration or the polymer MW is observed.

Figure 8a,b shows the Newtonian viscosities up to the maximum value as obtained from the Cross equation plotted vs the surfactant concentration. The viscosity increased progressively upon the surfactant addition, denoting enhanced interactions between the PE and the S. We can address that the viscosity increase of the plain polymer with added surfactant is the same for both JR30M and JR400 by 4 orders of magnitude. The SDBS surfactant (the surfactant with the lower cmc) gives the higher viscosity enhancement with the JR30M–S complexes at low surfactant concentration (up to 1 mM), while above 2 mM AOT the JR30M mixtures showed enhanced interaction and higher viscosities. Moreover, AOT–JR400 mixtures exhibit higher viscosities compared to those of the solutions of JR400–SDS or JR400–SDBS at the same surfactant concentration.

Our aim is to compare data from the different PE–S systems. Thus, the magnitude of the concentration dependence of the Newtonian viscosity with surfactant concentration can be expressed with the slope of the log–log plot as illustrated in Figure 8c,d. In particular, the slopes for the JR30M–surfactant systems are 2.2, 2.7, and 2.2 for the JR30M–SDS, JR30M–SDBS, and

JR30M–AOT complexes, respectively. Similarly, the slopes for the JR400–surfactant systems varies as 3.6, 3.3, and 4.3 for the JR400–SDS, JR400–SDBS, and JR400–AOT complexes, respectively.

The viscosities of viscoelastic pure surfactant solutions can be represented by a power law behavior of $\eta \sim (c/c^*)^z$ (where c^* marks the crossover concentration from the dilute to the semidilute solution) with $z > 3.5$.⁴⁷ However, other z values that have been observed are 8.5, 4.5, 3.5, 2.3, and 1.3.^{42,47–50} Cates and co-workers^{47–50} have proposed that for the lower exponents the structural relaxation time seems to be controlled by a combination of reptation and disentanglement processes. The high exponent (i.e., 8.5) was attributed to growth of micelles in the entanglement region above c^* and a pure reptation mechanism for the structural relaxation time. Hoffmann⁴⁷ explained the very low exponent of 1.3 by a kinetic process called diffusion-controlled bond interchange mechanism. The exponents ($\eta \sim c^z$) that have been observed for pure solutions of positive charged HEC derivatives with the same MW as the JR400 examined here were 0.6, 1.5, and 4.0 at high concentrations (up to 7 wt %) of PE.³⁹ Similar exponents between 3 and 5 have been reported for other charged HEC polymers.^{20,21,38} Recently, Tsianou and co-workers compared the binary mixture of oppositely charged and hydrophobically modified polyelectrolytes, which form physical networks by both electrostatic and hydrophobic interactions.³⁹ They have found that the network formed in such cases is reinforced due to enhanced hydrophobic associations and formation of mixed aggregates with the mixture viscosities being several orders of magnitude higher than those of each of the parent polymers alone at the same concentration. The scaling exponents for the concentration dependence of viscosity were a function of the mixing ratio and in the case of a positive excess polyion charge or close to the charge neutrality were as high as 10.6 and decreased down to 3.7 with a negative excess of polyion charge. These exponents are much higher than those of the single hydrophobically modified polyelectrolytes (0.5–1.5).³⁹

No clear distinction, however, of a mechanism could be noticed from the viscosity slopes of both PE–S mixtures. The higher slopes in the case of JR400–S complexes are probably analogous to the enhanced PE–S interactions due to the surfactant-dependent mechanism. A switch in the mechanism is observed for the JR30M–S complexes where it seems that the surfactant presence and architecture loses importance (weaker concentration dependence of viscosity) due to the polymer-controlled mechanism. The viscosity slopes of JR30M–S mixtures are within the experimental error the same even though the chemistry of the systems is very different. The higher slope (2.7) in the case of JR30M–SDBS, in comparison with that of the other JR30M–surfactants (2.2), possibly could be due to the variable branch length of this commercial surfactant. It is added that obviously the viscosity increase with the surfactant concentration must be also controlled by the electrostatic interactions of these oppositely charged polyelectrolyte–surfactant systems.

Comparison of Surfactants with Respect to Their Cmc.

A way to account for the different hydrophobic interactions of the different surfactants can be provided upon the normalization of the surfactant concentration with its respective cmc. Figure 9a,b shows the Newtonian viscosity changes for JR30M–S mixtures upon normal-

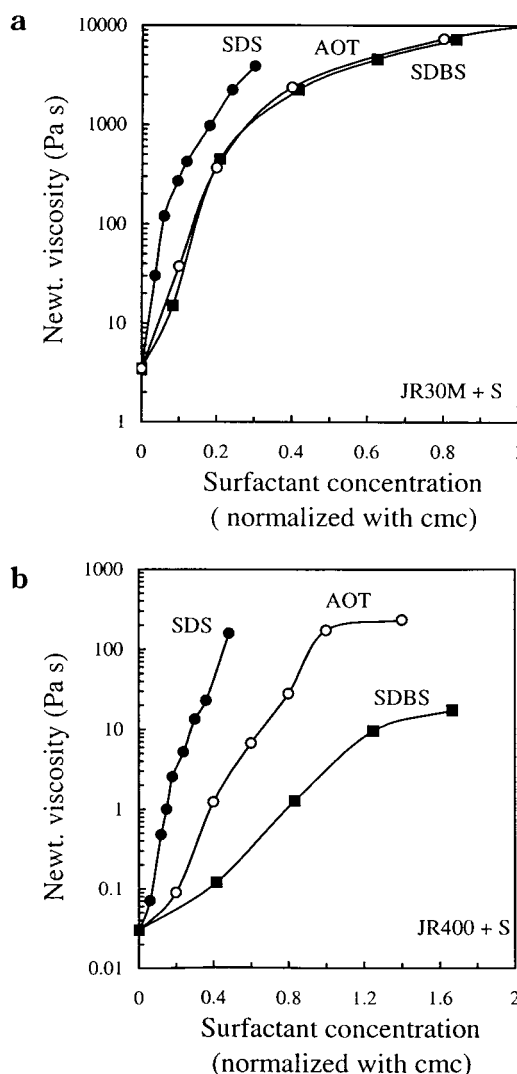


Figure 9. Changes in the Newtonian viscosities as a function of the normalized (with respect to cmc) surfactant concentration for (a) 1 wt % JR30M–surfactant systems and for (b) 1 wt % JR400–surfactant systems SDS (●), SDBS (■), and AOT (○).

ization of the surfactant concentration to their cmc. It is clear that, beyond 0.5 of the cmc in the JR30M–S mixtures (Figure 9a), further increase of surfactant does not affect the Newtonian viscosities. In this case further surfactant addition affects the number of micelles in the bulk but does not affect the number of JR30M–S cross-links. This is not the same in the case of JR400–S (Figure 9b) where the viscosities progressively increase with the surfactant addition, almost up to their nominal cmc (1.2 mM AOT and 2.5 mM SDBS). This is due to a surfactant-dependent association mechanism. SDS associates with the polyelectrolytes at much lower concentrations, normalized to its cmc, than the other surfactants. Apparently, SDS displays a much stronger affinity than for the other anionic surfactants, and thus, there are more aggregates at similar nominal concentration in comparison with the PE–SDBS and PE–AOT complexes. These affinity differences regarding hydrophobic interactions may also account for the differences in the values of the rheological parameters obtained for the PE–SDS complexes (lower Newtonian viscosities, higher critical shear rate, and lowest aggregate size). We anticipate, therefore, an even more complicated

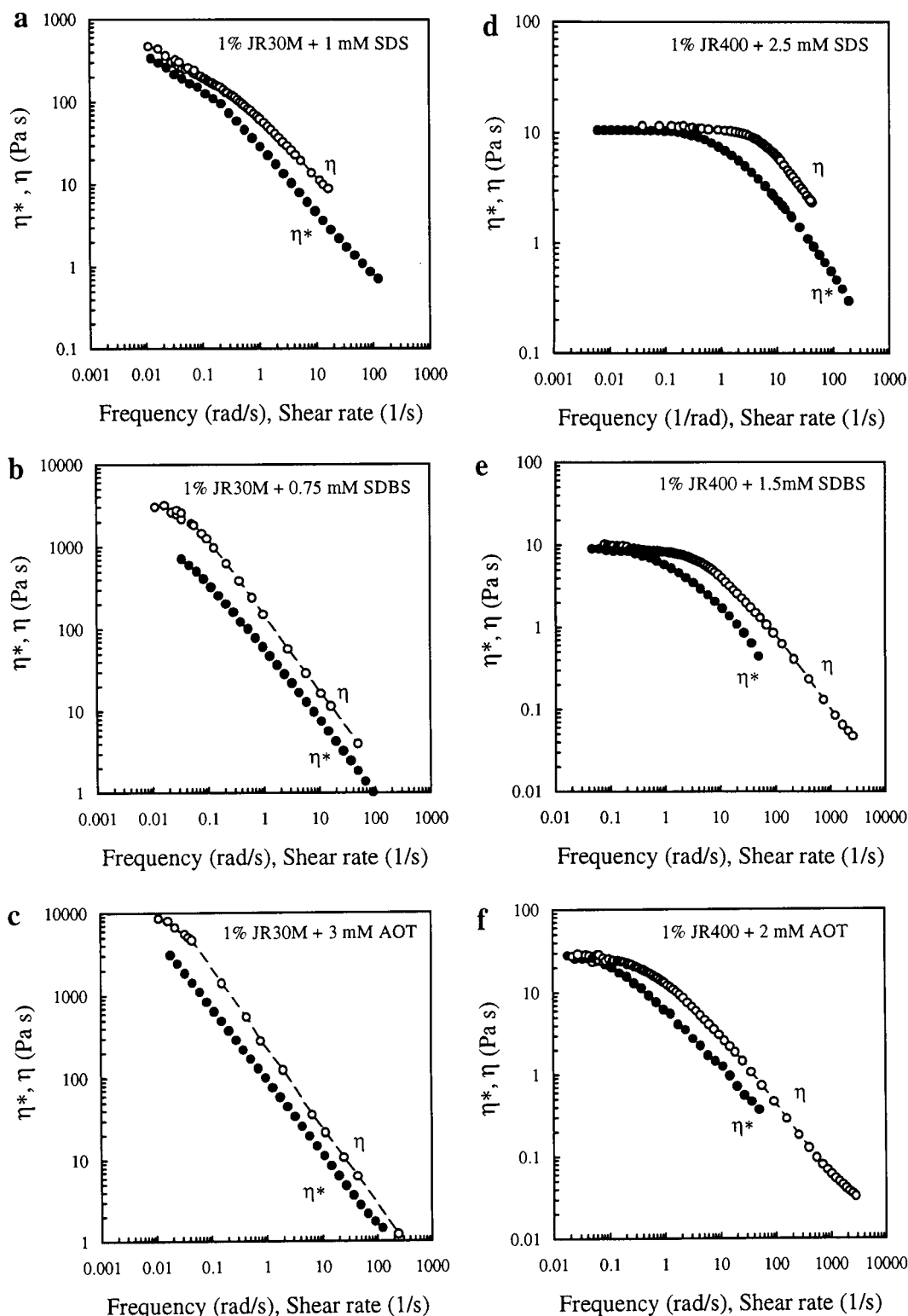


Figure 10. Testing of the Cox–Merz rule for polymer–surfactant systems: (●) complex viscosity η^* and (○) steady shear viscosity η . (a) 1 wt % JR30M with 1 mM SDS, (b) 1 wt % JR30M with 0.75 mM SDBS, (c) 1 wt % JR30M with 3 mM AOT, (d) 1 wt % JR400 with 2.5 mM SDS, (e) 1 wt % JR400 with 1.5 mM SDBS, and (f) 1 wt % JR400 with 2 mM AOT (0.5% strain, 25 °C).

situation where the size of the aggregated hydrophobic moieties may also affect the behavior of the mixture. For example, higher viscosities of PE–SDS complexes could be expected due to the high affinity of SDS and thus of the reinforcement effect of hydrophobic interactions; however, the viscosity can diminish from the disadvantage of the low aggregate size which is dependent on the surfactant architecture. Therefore, while the

viscosity changes demonstrate the importance of the electrostatic and hydrophobic interactions, it does not provide the complete picture of the association mechanism in these hydrophobic domains.

Cox–Merz Rule. One way to “support” the presence of aggregates of the above PE–S systems is to examine the validity of the Cox–Merz rule. According to this for equal values of oscillation frequency and shear rate, the

complex viscosity equals the steady shear viscosity. For ordinary polymers the empirical rule of Cox–Merz applies well, but this has not been fully explained theoretically. However, departure from the rule indicates that long-range interactions are present and that the intermolecular interactions are enthalpic rather than purely topological entanglements. Figure 10a–f illustrates the nonapplicability of the Cox–Merz rule for the mixtures of JR30M and JR400 polyelectrolytes with surfactants examined here. It is observed that with the high molecular weight polymer, and thus the high heterogeneity of aggregates, the complex viscosity (η^*) is lower than the dynamic viscosity (η) at all shear rates. The effect is less pronounced in the case of the low-MW JR400 where the departure from the rule is mostly effective at the high shear rate regime. Note that the differences appear more considerable when comparing the curves in linear scales. Hoffmann and co-workers⁵¹ also have found that HEC modified with hydrophobic or cationic groups with added surfactants exhibit different dynamic and shear viscosity, with the latter having higher values, as we have also observed in this study. However, the departure from the Cox–Merz rule in the case reported by Hoffmann et al. was substantially lower than that in our systems. They claimed that the network is built up of coiled polymeric chains that are connected through hydrophobic interactions of the surfactant molecules.

Further Considerations. *Polymer–Surfactant Effects.* The formation of a polymer–surfactant network with polymer–surfactant aggregates as physical entanglement points and the distribution of the surfactant between the “free” (solution) state and the aggregated state are supported by the data presented above. In this work we have tried to “separate” and “compare” the nature of the interactions, the binding mechanisms, and the structure of the complexes as affected by variables such as the structure of polymer and surfactant. It seems straightforward to decide which of the mechanisms is more effective. For the low molecular weight polymer the *surfactant effect* is responsible for the cooperativity of the cross-links. (Surfactant-dependent effects mean the effects apparently sensitive to the type of the three surfactants used.) However, less cooperative behavior and *polymer-dependent* cross-links are observed for the high molecular weight polymer–surfactant complexes (effects apparently sensitive to the type–MW of the two polymers used).

Gelling Efficiency. For the JR30M–S mixtures with low surfactant concentration addition (up to 1 mM), the gelling efficiency as measured from the G' at 1 Hz increases in the order SDBS > AOT \approx SDS (Figure 4). Therefore, the JR30M–SDBS association is stronger at low surfactant concentrations than that found for the other JR30M–S mixtures. However, beyond that concentration, addition of AOT or SDS on the high-MW polymer results to higher modulus, and the gelling efficiency follows the order AOT > SDS > SDBS. For the JR400–S systems the gelling efficiency increases in the order SDS > AOT \approx SDBS. The SDBS surfactant with the lower cmc (which is a descriptor of the tendency of the surfactant to associate) shows a lower association with the low-MW polymer than the other surfactants with higher cmc (in water).

An optimal elastic modulus at a frequency of 1 Hz could be observed at 2.5 mM SDS–JR30M, 3 mM SDBS–JR30M, and 3 mM SDBS, 3.5 mM AOT, and 4 mM SDS

with JR400. Above that concentration a decrease in the elastic modulus is obtained for both polymer systems. We cannot measure any decrease in the modulus for the other systems (JR30M–SDBS and JR30M–AOT) because these systems become biphasic upon further addition of surfactant. Thus, the complex solubility may influence the viscoelastic properties of polymer–surfactant complexes. The lower elastic moduli observed beyond the G' maximum in some of these PE–S systems probably do not reflect that the complexation process is diminished but may represent the formation of some “insoluble” complexes in mixture with soluble complexes. This lowering of G' may correspond to the surfactant concentration at which large PE–S “aggregates” start to dominate the system properties. Further addition of surfactant molecules may result in withdrawing from their normal role as binders in a continuous structure and affects the character of this matrix so that it could no longer give the same viscoelasticity. Nevertheless, possibly when the surfactant concentration exceeds some critical value, and with increasing number of aggregates, exclusion of surfactant segments from the “aggregate” space into the bulk might also occur. Note that the network formed by pure surfactant solutions could be an entangled network like it is assumed for polymer solutions, or it can be a connected network in which the micelles are fused together or are held together by adhesive contracts.⁵² Although our surfactants do not form such networks in aqueous solutions when no polymer is present, such network structures can form in PE–S mixtures since the cross-links originate from the surfactants. Moreover, micelle-like cross-links may be formed in some PE–S cases but not in others; for example, in the JR400–SDBS complexes notice the increase in elastic modulus between 1 and 2 mM of surfactant (Figure 4c) and the behavior of the PE–surfactant mixtures with respect to their cmc (Figure 9).

In PE–S systems in general, it is not clear whether the surfactant aggregates restructure upon binding, and how the polymer conformation changes upon binding. Although it is not in accordance with our flow measurements, probably as the number of adsorbed surfactant aggregates increases, the polymer chains may also undergo a change in response to the interaggregate electrostatic repulsion. Usually a contraction to the polymer conformation upon binding of surfactant is observed.^{9,53} In addition, coiling of the chains can also be expected both for electrostatic reasons, as polyelectrolyte chains in pure water are extended, and for topological reasons, i.e., to create a large contact area between the polymer chain and the (compact) micelle. Often associations between similarly charged or between charged and nonionic PE and surfactants are quite weak or absent mainly because of such unfavorable electrostatic repulsions.^{12,54}

Formation of “Aggregates”. The departure from the so-called Cox–Merz rule indicates that long-range interactions are present and supports presence of aggregates. The existence of aggregates, as well as whether they are comprised of units from one or more polymer chains, depends on the polymer molecular weight. Probably for the high molecular weight polymer the departure is substantial due to higher heterogeneity of the complexes combined with the stiff high-MW polymer chain entanglements and cross-linked bound aggregates. Similar behavior is observed for all JR30M–S

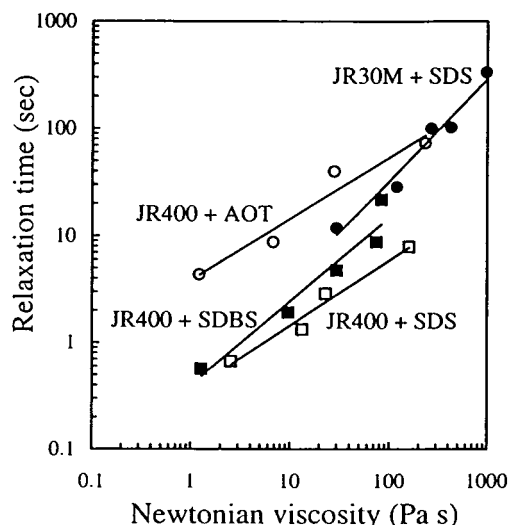


Figure 11. Double-log plot of the relaxation time (as measured by frequency oscillatory measurement) against Newtonian viscosities. 1 wt % JR400 with AOT (○), 1 wt % JR30M with SDS (●), 1 wt % JR400 with SDBS (■), and 1 wt % JR400 with SDS (□).

complexes; thus, the surfactant architecture is not important. At low-MW polymer the significant departure from the Cox–Merz rule occurs in the region of high shear rates, in the nonlinear regime. This deviation seems to hold in general in solutions of entangled macromolecules and is probably a consequence of shear-induced structural changes, leading to the formation of large-scale aggregate structures or a rather multiconnected network. The dynamic structure of defects formed at higher shear rates cannot reorganize rapidly on the time scale of experimental observation, but at lower shear rates this is the case. The differences between the low- and high-MW polymers are thus a result of a different dynamics of the complexes and not of the different structure.

It is reasonable to add that the differences in dynamic and flow properties of the systems observed (for example, Figure 4 with Figure 8) could be correlated to the above departure from the Cox–Merz rule. However, note that both PE–S systems exhibit a *single relaxation* process, the time constant of which increases continuously with the surfactant concentration. This time constant (as we observed from oscillation measurements) is identical with the structural relaxation time which determines the zero-shear viscosity as we have obtained from flow measurements. This is evident in the plot of the time constant from the oscillatory measurements against the Newtonian viscosity η (Figure 11). A single description of the relaxation time with increasing the Newtonian viscosity (and thus the surfactant concentration) confirms that both the oscillatory and flow responses result from a similar viscoelastic processes.

Lifetime of Aggregates. The factor determining the flow behavior in the zero shear rate limit is the lifetime of the intermolecular associations. The presence of the Newtonian flow behavior for the JR400–surfactant mixtures suggests that the time scale of the PE–S complex extension by shear is much longer for the low-MW polymer compared with the high MW, in accordance with the relaxation times presented in Figure 6. Thus, in the JR400–S complexes the cross-links can be easily stretched and are not strictly oriented, allow-

ing the additional adjustment of the aggregates at the Newtonian region. However, this is not valid in the case of the high chain entanglement and heterogeneous JR30M polymer–surfactant mixtures, where the viscosities of the solutions are practically non-Newtonian with the addition of the different surfactant types (*polymer-dependent effects*).

Critical Shear Rate. In the nonlinear domain the critical shear rate ($\dot{\gamma}_c$) at which the shear thinning occurs is dependent on the surfactant architecture and decreases in the order of surfactant SDS < SDBS < AOT for the JR400 polymer–surfactant system. The onset of such shear thinning can be considered as the relaxation time of the network structure under shear. Moreover, the evolution of this rheological parameter can be correlated to the growing size of the aggregates. It is well-known that the relaxation time τ_R is about $1/\dot{\gamma}_c$, so a decrease of $\dot{\gamma}_c$ gives a greater value of τ_R corresponding to a greater aggregate size. Physically the longer the aggregates, the easier is their alignment in the shear flow. Consequently, the aggregate sizes of JR400–surfactant systems increase in the order AOT > SDBS > SDS, and their relaxation time τ_R is an increasing function of the surfactant type (double tailed > partially branched and benzene ring > linear type lower chain length) in accordance with our observations from the relaxation behavior in dynamic oscillation (Figure 6). Such conclusions are not very obvious for the JR30M–surfactant complexes, and the overall structure presents a complex rheological response. Nevertheless, for individual JR30M– and JR400–surfactant systems the critical shear rate decreases with the increase of surfactant concentration.

Concluding Remarks

We report here on the gel formation and resulting rheological properties in aqueous solutions of cationic cellulose ether polymers of high and low molecular weight, upon the addition of anionic surfactants of different architecture but with the same charge. By comparing the rheological parameters of these complexes, such as the elastic modulus, the complex viscosities, Newtonian viscosities, the relaxation time, and the shear rate dependence, we assess the nature of the interactions leading to gel formation as well as structural properties of the polymer–surfactant aggregates.

In polyelectrolyte–oppositely charged surfactant complexes, the high-MW polyelectrolyte dominates the viscoelasticity of the complexes, while the surfactant architecture and the hydrophobic effect play a secondary role (*polymer-dependent cross-links*). *Surfactant-dependent cross-links* were obtained for the low-MW PE–S complexes, and the surfactant architecture markedly influences the dynamic properties and the Newtonian viscosity of the S–PE complexes. The *similarities* observed for the two molecular weight polyelectrolytes when we are changing the surfactant type keeping the same charge support the electrostatic nature of this cross-linking. The detailed chemistry of the surfactant is of no importance, and the formation of aggregates is affected by electrostatic interactions for both JR30M–S and JR400–S mixtures. The viscoelasticity is controlled by the behavior of these (charged) aggregates. We obtained the following: (i) The same complex viscosity and Newtonian viscosity slopes for the concentration dependence for each of the two polymers, independent of the surfactant architecture. The behavior of η^* and

η_{NW} must be controlled by the electrostatic interaction of the systems. (ii) The same slope of the elastic modulus at 1 Hz for the concentration dependence for both PE-S mixtures independent of the surfactant architecture. (iii) Taking into account that the modulus or the viscosity, which is a measure of the density of the entanglement points, is the result of entropic forces (as in normal viscoelastic network with entanglement or topological hindrances) and also of electrostatic interactions (as in real cross-linked networks), we can support that both entropic and energy elastic networks developed in oppositely charged PE-S. (iv) The common feature of all the systems is that they form "aggregates", and these aggregates are charged. We used the word aggregates to indicate the surfactant aggregates or polymer aggregates (caused by chain entanglement) or self-assemblies that form cross-links with the PE. (v) Departure from the Cox-Merz rule, with the shear rate viscosity higher by a factor of 2 from the oscillatory complex viscosity, independent of the surfactant architecture and the polymer MW. This behavior indicates a situation where the entangled network, upon deformation by shear, can relax faster to an undeformed state by a breaking and re-formation processes rather than by a reptation processes as in polymers. (vi) All polymer-surfactant complexes are viscoelastic and have a frequency dependence typical for networks containing entangled polymer chains. A general feature of these highly entangled systems is that a simple Maxwell model cannot be used to describe their viscoelastic properties. (vii) Both JR30M-S and JR400-S systems exhibit a single relaxation process, the time constant of which increases continuously with the surfactant concentration.

In addition to the similarities summarized above, a number of differences were observed which could be related to the polymer MW, to the surfactant architecture, and to the effect of the hydrophobic interactions. In particular: (i) The complexes of low-MW polyelectrolyte with oppositely charged surfactant have lower elastic modulus, lower complex and Newtonian viscosities, shorter relaxation times, and lower shear thinning behavior. (ii) The slopes from the log-log plot of the complex and Newtonian viscosities with surfactant concentration are higher in the case of JR400-S mixtures than those obtained for the high-MW PE-S systems. The higher concentration dependence of η and η^* of the JR400 mixtures in comparison to JR30M most probably reflects a more cooperative cross-linking behavior due to the surfactant effect. (iii) In the case of the high-MW polymer JR30M the surfactant presence and architecture lose importance, and a weaker concentration dependence of viscosity and a more cross-linked association are observed (higher viscosity and G'). This can be attributed to the polymer-dependent cross-links and chain entanglements, which are less subjected to the surfactant-controlled cross-link mechanism. (iv) The time scale for the association domains to detach from a mixed aggregate network (relaxation time, system dynamics) is governed by the molecular weight of the polymer and the type of surfactant (linear or double-tailed). The more asymmetric is the surfactant, the longer is the relaxation time. (v) There is almost no effect on the viscosity upon the addition of surfactant at a concentration above 50% of its cmc for the JR30M-S mixtures. This is not the case in the JR400-S systems where the viscosity increases up to 2 times the cmc,

denoting again a surfactant-controlled mechanism with the low-MW PE. Moreover, micelle-like cross-links may be formed in some PE-S cases but not in others. (vi) SDS displays a much stronger affinity and associates with the polymers at much lower concentrations, normalized to the cmc, than the other anionic surfactants. These affinity differences regarding hydrophobic interactions may also account for the differences in the values of the rheological parameters obtained for the SDS-PEs complexes (lower Newtonian viscosities, higher critical shear rate, and lowest aggregates size). (vii) The breaking of the aggregates on shear depends on the surfactant architecture and on the polymer MW. High critical shear rate is observed in the JR400-AOT systems in comparison with the JR400-SDS and JR400-SDBS mixtures. (viii) The differences in the Cox-Merz rule observed between the low- and high-MW polymers are a result of different dynamics of the complexes and not of different structures.

In conclusion, the use of rheological techniques provides further information and contributes to a more detailed picture of the polyelectrolyte behavior upon association with oppositely charged surfactants. Elucidation of these key relationships is likely to facilitate the design of specifically tailored rheology modifiers with improved application properties.

Acknowledgment. Financial support from the European Commission (I.S.C., Project No ERBFMBICT 972327) and the Swedish Natural Science Research Council, NFR (P.A.) is gratefully acknowledged. P.A. also acknowledges partial support from the U.S. National Science Foundation (CTS-9875848). We thank Ms. Sungsook Ahn for valuable help with the experiments and Dr. Marina Tsianou for helpful discussions. We thank Dr. Karl-Erik Bergqvist, Lund University, for performing the ^1H NMR experiment on SDBS. We also thank Prof. Andre Laschewsky (Université Catholique de Louvain) for pointing out the possibility of nonlinearity in the SDBS surfactant.

References and Notes

- (1) McCormick, C. L.; Bock, J.; Schulz, D. N. *Encyclop. Polym. Sci. Eng.* **1989**, *17*, 730.
- (2) *Industrial Water Soluble Polymers*; Finch, C. A., Ed.; Special Publication No. 186; The Royal Society of Chemistry: London, 1996.
- (3) Jönsson, B.; Lindman, B.; Holmberg, K.; Kronberg, B. *Surfactants and Polymers in Aqueous Solutions*; J. Wiley & Sons: Chichester, 1998.
- (4) Alexandridis, P. *Curr. Opin. Colloid Interface Sci.* **1996**, *1*, 490.
- (5) Iliopoulos, I. *Curr. Opin. Colloid Interface Sci.* **1998**, *3*, 493.
- (6) *Polyelectrolyte Gels*; Harland, R. S., Prud'homme, R. K., Eds.; ACS Symposium Series Vol. 480; American Chemical Society: Washington, DC, 1992.
- (7) *Interactions of Surfactants with Polymers and Proteins*; Goddard, E. D., Ananthapadmanabhan, K. P., Eds.; CRC Press: Boca Raton, FL, 1993.
- (8) Wei, Y.-C.; Hudson, S. M. *J. Macromol. Sci., Rev. Macromol. Chem. Phys.* **1995**, *C35*, 15.
- (9) Lindman, B.; Thalberg, K. In *Interactions of Surfactants with Polymers and Proteins*; Goddard, E. D., Ananthapadmanabhan, K. P., Eds.; CRC Press: Boca Raton, FL, 1993; p 203.
- (10) Kwak, J. C. T. *Polymer-Surfactant Systems*; Surfactant Science Series Vol. 77; Marcel Dekker: New York, 1998.
- (11) Morishima, Y.; Mizusaki, M.; Yoshida, K.; Dubin, P. L. *Colloids Surf. A: Physicochem. Eng. Aspects* **1999**, *147*, 149.
- (12) Goddard, E. D. *Colloids Surf.* **1986**, *19*, 301.
- (13) Hayakawa, K.; Kwak, J. C. T. In *Cationic Surfactants. Physical Chemistry*; Rubingh, D. N., Holland, P. M., Eds.; Marcel Dekker: New York, 1991; Chapter 5, p 189.

- (14) Efremov, V. A.; Khohlov, A. R.; Shikina, Yu. V. *Polym. Sci.* **1992**, *34*, 484.
- (15) Cabane, B.; Duplessix, R. *Colloids Surf.* **1985**, *13*, 19.
- (16) Takisawa, N.; Brown, P.; Bloor, D.; Hall, D. G.; Wyn-Jones, E. *J. Chem. Soc., Faraday Trans.* **1989**, *85*, 2099.
- (17) Triener, C.; Nguyen, D. *J. Phys. Chem.* **1990**, *94*, 2021.
- (18) Laschewsky, A. *Adv. Polym. Sci.* **1995**, *124*, 1.
- (19) Zakharova, Yu. A.; Kolbanovskiy, A. D.; Krinitskaya, L. A.; Kasaikin, V. A.; Wasserman, A. M. *Polym. Sci. Ser.* **1995**, *B37*, 439.
- (20) Kästner, U.; Hoffmann, H.; Döngess, R.; Ehrler, R. *Colloids Surf. A: Physicochem. Eng. Aspects* **1994**, *82*, 279.
- (21) Kästner, U.; Hoffmann, H.; Döngess, R.; Ehrler, R. *Colloids Surf. A: Physicochem. Eng. Aspects* **1996**, *112*, 209.
- (22) *Associative Polymers in Aqueous Media*; Glass, J. E., Ed.; ACS Symposium Series; American Chemical Society: Washington, DC, 2000.
- (23) Leung, P. S.; Goddard, E. D.; Han, C.; Glinka, C. J. *Colloids Surf.* **1985**, *13*, 47.
- (24) Goddard, E. D. *J. Soc. Cosmet. Chem.* **1990**, *41*, 23.
- (25) Tsianou, M.; Alexandridis, P. *Langmuir* **1999**, *15*, 8106.
- (26) Goddard, E. D.; Hannan, R. B. *J. Colloid Interface Sci.* **1976**, *55*, 73.
- (27) Piculell, L.; Lindman, B. *Adv. Colloid Interface Sci.* **1992**, *41*, 149.
- (28) Goddard, E. D.; Leung, P. S.; Padmanabhan, K. P. A. *J. Soc. Cosmet. Chem.* **1991**, *42*, 19.
- (29) Thalberg, K.; Lindman, B. *J. Phys. Chem.* **1989**, *93*, 1478.
- (30) Hansson, P.; Almgren, M. *Langmuir* **1994**, *10*, 2115.
- (31) Tsianou, M. Ph.D. Thesis, Lund University, Sweden, 1999.
- (32) Thuresson, K. Ph.D. Thesis, Lund University, Sweden, 1996.
- (33) Harrison, I. M.; Meadows, J.; Robb, I. D.; Williams, P. A. *J. Chem. Soc., Faraday Trans.* **1995**, *91*, 3919.
- (34) Elworthy, P. H.; Mysels, K. J. *J. Colloid Sci.* **1966**, *21*, 331.
- (35) Greshman, J. W. *J. Phys. Chem.* **1957**, *61*, 581.
- (36) Williams, E. F.; Woodbury, N. T.; Dixon, J. K. *J. Colloid Sci.* **1957**, *12*, 452.
- (37) Goddard, E. D.; Leung, P. S. *Colloids Surf.* **1992**, *65*, 211.
- (38) Hoffmann, H.; Kästner, U.; Döngess, R.; Ehrler, R. *Polym. Gels Networks* **1996**, *4*, 509.
- (39) Tsianou, M.; Thuresson, K.; Lindman, B., submitted.
- (40) Drye, T. J.; Cates, M. E. *J. Chem. Phys.* **1992**, *96*, 1367.
- (41) Galatanu, N.; Chronakis, I. S.; Angel, D. F.; Khan, A. *Langmuir* **2000**, *16*, 4922.
- (42) Turner, M. S.; Marques, C.; Cates, M. E. *Langmuir* **1993**, *9*, 695.
- (43) Hansson, P. Ph.D. Thesis, Uppsala University, Sweden, 1996.
- (44) Molyneux, P. *Water-Soluble Synthetic Polymers: Properties and Behavior*; CRC Press: Boca Raton, FL, 1984; Vol. 2, Chapter 1.
- (45) Noda, I.; Tsuge, T.; Nagasawa, M. *J. Phys. Chem.* **1970**, *74*, 710.
- (46) Whorlow, R. W. *Rheological Techniques*; Ellis Horwood: London, 1992.
- (47) Hoffmann, H. In *Structure and Flow in Surfactant Solutions*; Herb, C. A., Prud'homme, R. K., Eds.; ACS Symposium Series 578; American Chemical Society: Washington, DC, 1994.
- (48) Turner, M. S.; Cates, M. E. *J. Phys. II* **1992**, *2*, 503.
- (49) Cates, M. E. *J. Phys. (Paris)* **1988**, *49*, 1513.
- (50) Cates, M. E. *Macromolecules* **1987**, *20*, 2289.
- (51) Hoffmann, H.; Hoffmann, S.; Kästner, U. *Adv. Chem. Ser.* **1996**, *248*, 219.
- (52) Appell, J.; Porte, G.; Khatory, A.; Kern, F.; Candau, S. *J. Phys. II* **1992**, *2*, 1045.
- (53) Chandar, P.; Somasundaran, P.; Turrro, N. J. *Macromolecules* **1988**, *21*, 950.
- (54) Methemitis, C.; Morcellet, M.; Sabbadin, J.; Francois, J. *Eur. Polym. J.* **1986**, *22*, 619.

MA000609K